This article was downloaded by: [Renmin University of China]
On: 13 October 2013, At: 10:46
Publisher: Taylor & Francis
Informa Ltd Registered in England and Wales Registered Number: 1072954 Registered office: Mortimer House, 37-41 Mortimer Street, London W1T 3JH, UK

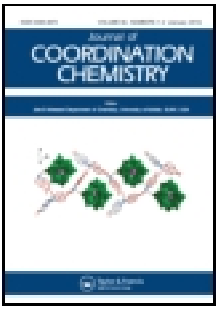

Journal of Coordination Chemistry
Publication details, including instructions for authors and subscription information:
http://www.tandfonline.com/loi/gcoo20

Non-oxo vanadium(IV) complexes with acetylacetone 4-R-benzoylhydrazones

KOPPANATHI NAGARAJU [a], ANINDITA SARKAR [a] & SAMUDRANIL PAL [a]

[a] School of Chemistry, University of Hyderabad, Hyderabad, India

Accepted author version posted online: 07 Nov 2012.Published online: 12 Dec 2012.

To cite this article: KOPPANATHI NAGARAJU, ANINDITA SARKAR & SAMUDRANIL PAL (2013) Non-oxo vanadium(IV) complexes with acetylacetone 4-R-benzoylhydrazones, Journal of Coordination Chemistry, 66:1, 77-88, DOI: 10.1080/00958972.2012.747089

To link to this article: http://dx.doi.org/10.1080/00958972.2012.747089

PLEASE SCROLL DOWN FOR ARTICLE

Taylor & Francis makes every effort to ensure the accuracy of all the information (the “Content”) contained in the publications on our platform. However, Taylor & Francis, our agents, and our licensors make no representations or warranties whatsoever as to the accuracy, completeness, or suitability for any purpose of the Content. Any opinions and views expressed in this publication are the opinions and views of the authors, and are not the views of or endorsed by Taylor & Francis. The accuracy of the Content should not be relied upon and should be independently verified with primary sources of information. Taylor and Francis shall not be liable for any losses, actions, claims, proceedings, demands, costs, expenses, damages, and other liabilities whatsoever or howsoever caused arising directly or indirectly in connection with, in relation to or arising out of the use of the Content.

This article may be used for research, teaching, and private study purposes. Any substantial or systematic reproduction, redistribution, reselling, loan, sub-licensing, systematic supply, or distribution in any form to anyone is expressly forbidden. Terms & Conditions of access and use can be found at http://www.tandfonline.com/page/terms-and-conditions

Journal of Coordination Chemistry
Vol. 66, No. 1, 10 January 2013, 77–88

Non-oxo vanadium(IV) complexes with acetylacetone 4-*R*-benzoylhydrazones

KOPPANATHI NAGARAJU, ANINDITA SARKAR and SAMUDRANIL PAL*

School of Chemistry, University of Hyderabad, Hyderabad, India

(*Received 20 July 2012; in final form 20 September 2012*)

Vanadium(IV) complexes of formula [V(ac*R*bh)$_2$] with acetylacetone 4-*R*-benzoylhydrazones (H$_2$ac*R*bh, *R*=H, Cl, OMe and NO$_2$) have been synthesized and characterized by elemental analysis, IR, UV–vis, and electron paramagnetic resonance (EPR) spectroscopic measurements. All the complexes are one-electron paramagnetic and show very similar axial EPR spectra in frozen solution. In dimethylformamide, the complexes display a V(IV)−V(III) redox couple in the $E_{1/2}$ range −0.16–−0.25 V (*versus* Ag/AgCl). Single crystal X-ray structures of [V(ac*H*bh)$_2$] and [V(ac*Cl*bh)$_2$] have been determined. The metal center in each complex is in a distorted trigonal prismatic N$_2$O$_4$ coordination sphere assembled by the enolate-O, the imine-N, and the iminolate-O donor ac*R*bh^{2-}.

Keywords: Non-oxo vanadium(IV); Aroylhydrazones; Crystal structures; Trigonal prism; Physical properties

1. Introduction

Continuing interest in the coordination chemistry of vanadium stems from its involvement in several biological systems [1–8] and the applications of its complexes in areas such as organic synthesis, catalysis, and medicinal chemistry [7–18]. As a result, vast literature on vanadium chemistry and its complexes is available [1–18]. However, compared to non-oxo vanadium(IV/V), oxovanadium(IV/V) species are dominant in this literature, due to stability of the oxovanadium(IV/V) complexes and the ease of their formation under aerobic and wet conditions. In contrast, non-oxo vanadium(IV/V) complexes [19–28] are generally synthesized in strictly anaerobic and dry conditions. There are few reports on formation of non-oxo vanadium(IV) species using starting materials such as [V(acac)$_3$], [V(acac)$_2$Cl$_2$], or [V(bzac)$_2$Cl$_2$] (acac$^-$ = acetylacetonate and bzac$^-$ = benzoylacetonate) in ambient atmosphere [29–31]. However, these non-oxo starting materials themselves are prepared in anaerobic and dry conditions. Such non-oxo vanadium centers occur in biological systems, namely amavanadin [3] and vanadium nitrogenase [4]. We have been working on the coordination chemistry of vanadium with Schiff bases derived from acid hydrazides and related systems for the last several years [32–42]. [VO(acac)$_2$] is a popular precursor [15] for synthesis of new oxovanadium(IV/V) complexes. We have observed that [VO(acac)$_2$] with tridentate dianionic ligands under aerobic conditions in methanol provides

---

*Corresponding author. Email: spsc@uohyd.ernet.in

Journal of Coordination Chemistry
ISSN 0095-8972 print/ISSN 1029-0389 online © 2012 Taylor & Francis
http://dx.doi.org/10.1080/00958972.2012.747089

$\{VO(OMe)\}^{2+}$ [32,39,40], while complexes of the $\{OV(\mu\text{-}O)VO\}^{4+}$ core are obtained when the reaction medium is changed to acetonitrile [33,39,40]. Tridentate mono-anionic ligands produce complexes of $\{VO_2\}^{+}$ in acetonitrile under aerobic conditions [34–36,38]. In all these instances, both acetylacetonates of $[VO(acac)_2]$ are replaced by methoxo/oxo groups (from the reaction medium) and the tridentate ligand. In methanol only, one acetylacetonate of $[VO(acac)_2]$ is replaced by tridentate mono-anionic ligands and mixed ligand complexes of $\{VO\}^{2+}$ are obtained [37]. Both $\{VO(OMe)\}^{2+}$ and $\{VO_2\}^{+}$ containing species are monomeric if the metal center is trigonal-bipyramidal, whereas they form dimeric units via weak equatorial-apical bridging if the metal center is square pyramidal. Equimolar amounts of $[VO(acac)_2]$ and preformed Schiff bases have been used in all the above syntheses except for one case [40]. In this exception, $[VO(acac)_2]$ was treated directly with equimolar amounts of aroylhydrazines in air resulting in formation of $\{VO(OMe)\}^{2+}$ (in methanol) and $\{OV(\mu\text{-}O)VO\}^{4+}$ (in acetonitrile) with the tridentate ligands generated by template condensation of $acac^{-}$ and aroylhydrazines [40]. Similar reactions of $[VO(acac)_2]$ and aroylhydrazines, namely benzoylhydrazine and salicyloylhydrazine in 1 : 2 mol ratio in dry methanol under dinitrogen, produce non-oxo vanadium(IV) complexes of tridentate deprotonated acetylacetone aroylhydrazones (scheme 1) [19]. Isolation of the same species as a byproduct was reported later in the reaction of equimolar amounts of the non-oxo starting material $[V(acac)_3]$ and salicyloylhydrazine in 95% ethanol under aerobic conditiond [29]. We have observed that the same non-oxo vanadium(IV) species can be synthesized in moderate yields from $[VO(acac)_2]$, 4-*R*-benzoylhydrazines (R = H, Cl, OMe, and NO_2), and acetylacetone (in 1 : 2 : 1 mol ratio) using normal solvent under aerobic conditions (scheme 1). Herein, we describe the synthesis of these complexes having the general formula $[V(acRbh)_2]$ (H_2acRbh = enol form of acetylacetone aroylhydrazone) and their physical properties. X-ray structures of two complexes where R = H and Cl are also reported.

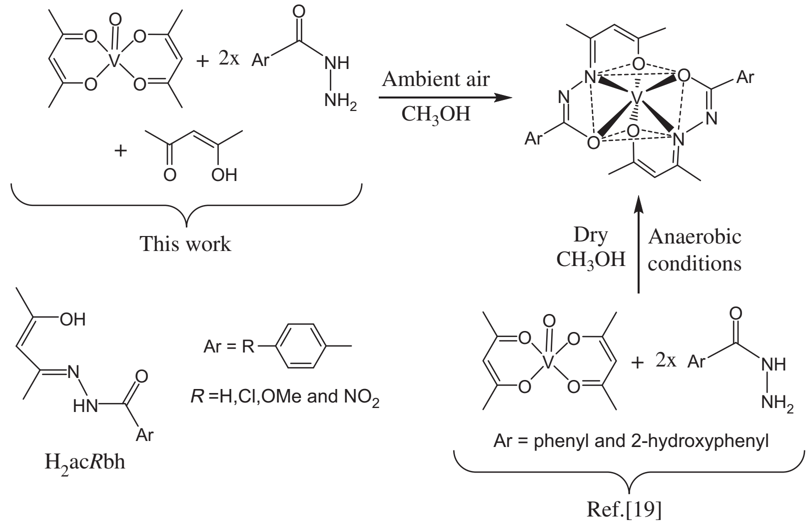

Scheme 1. The Schiff base H_2acRbh and the synthetic routes for $[V(acRbh)_2]$.

2. Experimental

2.1. *Materials*

Bis(acetylacetonato)oxovanadium(IV) was prepared by following a reported procedure [43]. All other chemicals and solvents used in this work were of analytical grade available commercially and were used as received.

2.2. *Physical measurements*

Elemental (C, H, and N) analysis data were obtained with a Thermo Finnigan Flash EA1112 series elemental analyzer. Solution electrical conductivities were measured using a Digisun DI-909 conductivity meter. Magnetic susceptibility measurements were performed with a Sherwood Scientific balance. Diamagnetic corrections calculated from Pascal's constants [44] were used to obtain the molar paramagnetic susceptibilities. Infrared spectra were recorded on a Jasco-5300 FTIR spectrophotometer. A Shimadzu UV-3600 UV–vis–near-infrared spectrophotometer was used to collect the electronic spectra. X-band electron paramagnetic resonance (EPR) measurements were performed on a Jeol JES-FA200 spectrometer. A CH Instruments model 620A electrochemical analyzer was used for cyclic voltammetric measurements with dimethylformamide solutions of the complexes containing tetrabutylammonium perchlorate as the supporting electrolyte. The three-electrode measurements were carried out at 298 K under dinitrogen with a platinum working electrode, a platinum wire auxiliary electrode and an Ag/AgCl reference electrode. Under identical conditions, the $E_{1/2}$ value of the Fc^+/Fc couple was observed at 0.68 V. The potentials reported in this work are uncorrected for junction contributions.

2.3. *Synthesis of the complexes [V(acRbh)$_2$]*

All complexes were prepared using the following general procedure: an acetonitrile solution (15 mL) of 4-*R*-benzoylhydrazine (3.0 mmol) was added to an acetonitrile solution (15 mL) of [VO(acac)$_2$] (400 mg, 1.5 mmol) and acetylacetone (185 mg, 190 µL, 1.5 mmol). The mixture was boiled under reflux for 2 h. The dark purple reaction mixture was then concentrated to ~8-10 mL on a steam bath and cooled to room temperature. The complex deposited as dark crystalline material was collected by filtration and dried in air.

2.3.1. [V(ac*H*bh)$_2$] (1). Yield: 265 mg (37%). Anal. Calcd for $VC_{24}H_{24}N_4O_4$: C, 59.61; H, 5.01; N, 11.59. Found: C, 59.44; H, 4.87; N, 11.45. μ_{eff} (μ_B) at 298 K: 1.98. Selected IR bands (cm^{-1}): 1586 (m), 1541 (s), 1495 (m), 1441 (s) 1366 (s), 1319 (s), 1170 (w), 1142 (m), 1069 (m), 1020 (s), 951 (s), 864 (m), 795 (s), 783 (s), 702 (s), 683 (s), 619 (m), 594 (s), 490 (s), 432 (s). UV–vis data (λ_{max} (nm) (ε (M^{-1} cm^{-1}))): 1010 (47), 540 (5.7×10^3), 325 (32.8×10^3), 250 (37.9×10^3).

2.3.2. [V(ac*Cl*bh)$_2$] (2). Yield: 315 mg (38%). Anal. Calcd for $VC_{24}H_{22}N_4O_4Cl_2$: C, 52.17; H, 4.02; N, 10.15. Found: C, 51.86; H, 3.89; N, 10.34. μ_{eff} (μ_B) at 298 K: 1.80. Selected IR bands (cm^{-1}): 1593 (m), 1539 (s), 1489 (m), 1445 (w), 1400 (m), 1362 (s), 1316 (s), 1167 (w), 1144 (m), 1088 (s), 1034 (w), 1011 (m), 951 (m), 843 (s), 799 (m), 737 (s), 710 (m), 683 (m), 627 (m), 604 (s), 517 (w), 498 (w), 476 (m), 463 (w), 432 (m). UV–vis data (λ_{max} (nm) (ε ($M^{-1}\,cm^{-1}$))): 1010 (55), 545 (3.8×10^3), 330 (24.6×10^3), 255 (30.8×10^3).

2.3.3. [V(ac*OMe*bh)$_2$] (3). Yield: 280 mg (34%). Anal. Calcd for $VC_{26}H_{28}N_4O_6$: C, 57.44; H, 5.20; N, 10.31. Found: C, 57.12; H, 4.99; N, 10.02. μ_{eff} (μ_B) at 298 K: 1.88. Selected IR bands (cm^{-1}): 1606 (s), 1543 (s), 1508 (s), 1418 (s), 1367 (s), 1304 (s), 1250 (s), 1167 (s), 1102 (m), 1028 (s), 949 (m), 841 (m), 789 (w), 747 (m), 708 (w), 635 (s), 475 (m), 430 (m). UV–vis data (λ_{max} (nm) (ε ($M^{-1}\,cm^{-1}$))): 1010 (56), 550 (4.5×10^3), 330 (33.3×10^3), 270 (35.0×10^3).

2.3.4. [V(ac*NO$_2$*bh)$_2$] (4). Yield: 320 mg (37%). Anal. Calcd for $VC_{24}H_{22}N_6O_8$: C, 50.25; H, 3.87; N, 14.66. Found: C, 49.85; H, 3.69; N, 14.29. μ_{eff} (μ_B) at 298 K: 1.82. Selected IR bands (cm^{-1}): 1599 (m), 1547 (s), 1518 (m), 1495 (m), 1430 (m), 1406 (m), 1339 (s), 1308 (s), 951 (m), 864 (m), 845 (m), 793 (m), 704 (s), 602 (s), 509 (m), 469 (m), 430 (w). UV–vis data (λ_{max} (nm) (ε ($M^{-1}\,cm^{-1}$))): 1010 (51), 550 (4.5×10^3), 390 (30.6×10^3), 275 (65.4×10^3).

2.4. *X-ray crystallography*

X-ray quality single crystals of [V(ac*H*bh)$_2$] (**1**) and [V(ac*Cl*bh)$_2$] (**2**) were obtained directly from the corresponding reaction mixture. Unit cell parameters and intensity data for **1** and **2** were obtained at 298 K on a Bruker–Nonius SMART APEX CCD single crystal diffractometer equipped with a graphite monochromator and a Mo K$_\alpha$ fine-focus sealed tube ($\lambda = 0.71073$ Å) operated at 2.0 kW. In each case, the detector was placed at a distance of 6.0 cm from the crystal. Data were collected with a scan width of 0.3° in ω and an exposure time of 15 s/frame. Data acquisition and data extraction were performed with SMART and the SAINT-Plus software [45], respectively. SADABS [46] was used for absorption correction. Both structures were solved by direct methods and refined on F^2 by full-matrix least-squares procedures. All nonhydrogen atoms were refined anisotropically. Hydrogens were included in the structure factor calculation at idealized positions by using a riding model. The SHELX-97 programs [47] available in the WinGx package [48] were used for structure solution and refinement. The ORTEX6a [49] and Platon [50] packages were used for molecular graphics. Significant crystallographic data are listed in table 1.

3. Results and discussion

3.1. *Synthesis*

Reactions of [VO(acac)$_2$], 4-*R*-benzoylhydrazines and acetylacetone in 1 : 2 : 1 mol ratio in acetonitrile under aerobic conditions provide [V(ac*R*bh)$_2$] (**1–4**) in 34–38% yields (scheme 1). Similar yields without any significant improvement were observed when the reactions were performed in dry acetonitrile and under dinitrogen. If the reactions were

Table 1. Crystallographic data[a] for [V(ac*H*bh)$_2$] (**1**) and [V(ac*Cl*bh)$_2$] (**2**).

Complex	**1**	**2**
Empirical formula	$VC_{24}H_{24}N_4O_4$	$VC_{24}H_{22}N_4O_4Cl_2$
Formula weight	483.41	552.30
Crystal system	Monoclinic	Monoclinic
Space group	$P2_1/c$	$P2_1/c$
Unit cell dimensions (Å, °)		
a	8.9050(5)	9.0707(7)
b	11.8590(7)	11.5888(9)
c	22.4544(14)	23.8327(18)
β	97.786(1)	91.601(1)
Volume (Å^3), Z	2349.4(2), 4	2504.3(3), 4
Calculated density ρ (g cm^{-3})	1.367	1.465
Absorption coefficient μ (mm^{-1})	0.460	0.648
Crystal size (mm^3)	0.42 × 0.35 × 0.12	0.38 × 0.04 × 0.04
θ Range for data collection (°)	1.83–26.02	1.71–26.06
Reflections collected/unique	22,983/4624	16,181/4923
Reflections $[I \geq 2\sigma(I)]$	3683	3342
Data/restraints/parameters	4624/0/302	4923/0/320
Final R indices $[I \geq 2\sigma(I)]$	$R_1 = 0.0495$, $wR_2 = 0.1191$	$R_1 = 0.0531$, $wR_2 = 0.1223$
R indices (all data)	$R_1 = 0.0643$, $wR_2 = 0.1278$	$R_1 = 0.0852$, $wR_2 = 0.1363$
Goodness-of-fit on F^2	1.039	1.034
Largest difference peak and hole (e Å^{-3})	0.518 and −0.214	0.393 and −0.205

[a]The data reported previously for **1** [19]: $a = 8.906(3)$ Å, $b = 11.840(2)$ Å, $c = 22.450(6)$ Å, $\beta = 97.72(3)°$, $V = 2345.8$ Å^3, $R = 0.102$, $Rw = 0.099$, Largest difference peak = 1.46 e Å^{-3}.

performed in acetonitrile or in methanol under aerobic condition without free acetylacetone, the complexes have been isolated in relatively much lower yields (~15–20%). Perhaps, excess acetylacetone facilitates protonation of the metal-bound oxo group and the eventual displacement of the coordinated water by one of the donors of the tridentate (ac*R*bh^{2-}) formed by template condensation of acetylacetonate and 4-*R*-benzoylhydrazine [28,51]. Elemental analysis data for **1–4** support the general molecular formula [V(ac*R*bh)$_2$]. The room temperature solid-state magnetic moments of the complexes are 1.80–1.98 μ_B, consistent with the one-electron paramagnetic nature and hence, the +4 oxidation state of vanadium in **1–4**. Ligands derived from acetylacetone and hydrazine derivatives are known to behave as noninnocent [52]. However, the EPR characteristics (*vide infra*) rule out any significant noninnocent character of the ligands in **1–4**. All the complexes are sparingly soluble in methanol, moderately soluble in acetonitrile, and highly soluble in dimethylformamide and chlorinated solvents. All these solvents provide purple solutions of **1–4** and in solution, they are nonelectrolytes.

3.2. *Spectroscopic properties*

Infrared spectra of **1–4** were collected by using KBr pellets. The spectra display a large number of bands of various intensities from 1610 to 400 cm^{-1}. Except for the following few we have not attempted to assign all the bands. The C=N stretch appears as a medium to strong band at 1607–1586 cm^{-1} [32–42]. Three more medium to strong bands at ~1545, ~1500, and ~1440 cm^{-1} are possibly associated with the aromatic ring of the ligands [53]. Complex **4** displays two additional bands at 1558 and 1339 cm^{-1} due to the asymmetric and the symmetric stretches of the nitro substituent of the ligand [53].

Dichloromethane solutions of **1–4** were used to record the electronic spectra. The spectral profiles of all four complexes are very similar except for some shifts of band positions. A representative spectrum is depicted in figure S1 (Supplementary material). The spectra display a very weak shoulder at ~1010 nm, a broad strong band at 550–540 nm and two very strong bands at 390–325 and 275–250 nm. The lowest energy weak shoulder is attributed to a d–d transition [54]. Absorptions in the visible region with medium to large molar extinction coefficients are fairly common for non-oxo vanadium(IV) complexes and are primarily due to ligand-to-metal charge transfer (LMCT) transitions [20, 51, 54]. Thus, of the three strong absorptions observed, the first two are assigned to LMCT transitions and the highest energy band is believed to be due to a ligand-centered transition (figure S1).

The EPR spectra of **1–4** were recorded using solutions in dichloromethane-toluene (1 : 1). All the room temperature (298 K) fluid phase spectral profiles are very similar. Similarly, the frozen solution (125 K) spectra are also indistinguishable and typical of mononuclear vanadium(IV) species with approximately axial symmetry. The spectra of **2** at 298 and 125 K are shown in figure 1. The *g*-values and the hyperfine constants (A) calculated from these spectra are listed in table 2. Room temperature spectra display an isotropic eight-line hyperfine pattern with $g_{\mathrm{iso}} \approx 1.97$ ($A_{\mathrm{iso}} \approx 69 \times 10^{-4}\,\mathrm{cm}^{-1}$), while an axial pattern with $g_{\|} \approx 1.96$ ($A_{\|} \approx 126 \times 10^{-4}\,\mathrm{cm}^{-1}$) and $g_{\perp} \approx 1.99$ ($A_{\perp} \approx 55 \times 10^{-4}\,\mathrm{cm}^{-1}$) was observed in the 125 K spectra. The g_{av} value of ≈ 1.98 (calculated using the expression $g_{\mathrm{av}} = (g_{\|} + 2g_{\perp})/3$) is very close to the g_{iso} value obtained from the room temperature spectral pattern. However, the A_{av} value of $\approx 79 \times 10^{-4}\,\mathrm{cm}^{-1}$ (calculated using the expression $A_{\mathrm{av}} = (A_{\|} + 2A_{\perp})/3$) is slightly larger than the A_{iso} value calculated from the room temperature spectra. Depending upon the coordination geometry and the ground state, six-coordinate vanadium(IV) species display two types of axial EPR spectra. Distorted octahedral complexes with d_{xy} ground state display $g_{\|} < g_{\perp} \sim 2.0$ and $A_{\|} >> A_{\perp}$, while the opposite relations $g_{\perp} < g_{\|} \sim 2.0$ and $A_{\perp} >> A_{\|}$ are distinctive for trigonal prismatic complexes with the d_{z2} ground state [51, 54–63]. However, the *g*- and *A*-values (table 2) of trigonal prismatic **1–4** (*vide infra*) do not reflect the relations typical of their geometry. The EPR spectral behavior of **1** was studied in detail before [55,56]. The spectra of the present complexes including **1** are essentially identical with the reported spectrum of **1** in frozen dichloromethane-toluene (1 : 1) solution [56]. By simulating the spectrum of **1,** a slight anisotropy was detected in the *g* component and the g_1, g_2, and g_3 were reported as 1.957, 1.983, and 1.979, respectively, with the corresponding $|A_1|$, $|A_2|$, and $|A_3|$ values as 126.6×10^{-4}, 54.8×10^{-4}, and $13.7 \times 10^{-4}\,\mathrm{cm}^{-1}$, respectively [56]. Using these parameters and the *g* tensor, it was suggested that the unpaired electron in **1** occupies an orbital which is ~ 90% metal (78% d_{z^2}, 10% $d_{x^2-y^2}$ and 2% 4s) and $\leq$ 10% ligand in character instead of the pure d_{z^2} as commonly observed for trigonal prismatic non-oxo vanadium (IV) complexes.

3.3. *Description of X-ray structures*

The X-ray structure of **1** synthesized under anaerobic conditions was reported earlier [19]. However, we have determined the structure of **1** again. The quality of the present structure is better than that of the previously reported structure. We have also determined the structure of **2** for comparison. Despite our best effort, X-ray quality single crystals of **3** and **4** could not be grown. However, the presence of the substituent Cl in **2** does not induce any significant difference in its structure compared to the structure of **1** (*vide infra*).

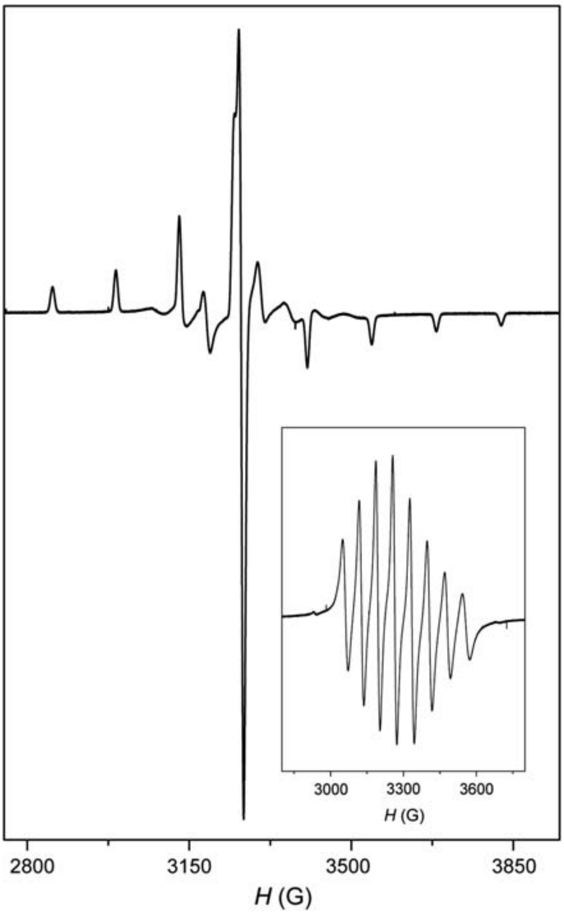

Figure 1. The EPR spectra of dichloromethane–toluene (1 : 1) solution of [V(ac*Cl*bh)$_2$] (**2**) in frozen condition (125 K) and in fluid phase (298 K) (inset).

Table 2. The EPR parameters[a] and redox potentials[b] for **1**–**4**.

Complex	g_{iso} (A_{iso})	$g_{\parallel}$ ($A_{\parallel}$)	$g_{\perp}$ ($A_{\perp}$)	$E_{1/2}$ (V) (ΔE_p (mV))
1	1.97 (69)	1.96 (126)	1.99 (55)	−0.22 (110)
2	1.97 (68)	1.96 (126)	1.99 (55)	−0.18 (120)
3	1.97 (69)	1.96 (127)	1.98 (55)	−0.25 (130)
4	1.98 (69)	1.96 (126)	1.99 (55)	−0.16 (110), −1.04 (240)

[a] The A values are in 10^{-4} cm^{-1}.
[b] $E_{1/2} = (E_{pa} + E_{pc})/2$, $\Delta E_p = E_{pa} - E_{pc}$.

Molecular structures of **1** and **2** with atom labeling schemes are shown in figure 2. Selected bond parameters associated with the metal centers are listed in table 3. In both complexes, ac*R*bh^{2-} is tridentate through iminolate–O, the imine–N, and the enolate–O. The C−O and the C−N bond lengths in the –C(O)N− fragments of the ligands in **1** and **2** are 1.312(3)−1.319(3) and 1.289(4)−1.298(3) Å, respectively. These values are consistent with the deprotonated form of the O-coordinated amide functionalities [19,29,32–36,38,40,42,52,64–67]. The C−O (1.280(4)−1.294(4) Å) and the C−C (1.373(5)−1.379(5) Å) bond lengths in the –C(O)C− fragments of the ligands are also within the corresponding bond length ranges found in O-coordinated enolate functionalities [19,29,37,40–42,52,66]. The V−O(iminolate), the V−N(imine), and the V−O(enolate) bond lengths are very similar in **1** and **2** (table 3) and comparable with the bond lengths reported for vanadium(IV) complexes having the same coordinating atoms [19,29,37,41,42]. The N_2O_4 coordination sphere assembled by the two ligands in **1** and **2** is a distorted trigonal prism (figure 3). The two five-membered chelate rings formed by the iminolate–O and the imine–N are along the two opposite edges of a tetragonal face, while the six-membered chelate rings formed by the imine–N and the enolate–O are along the two diagonally opposite edges of the two trigonal faces (figure 2). The extents of distortion from the ideal trigonal prismatic coordination sphere in the two structures are very similar. The edge lengths of the trigonal faces in **1** and **2** are 2.63−2.76 and 2.63−2.73 Å, respectively,

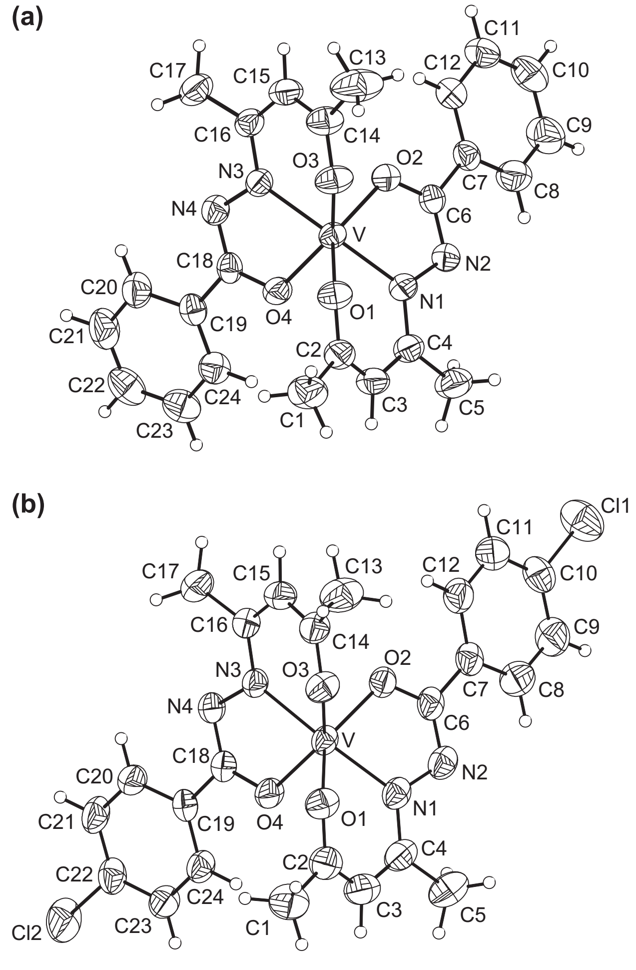

Figure 2. The molecular structures of (a) [V(ac*H*bh)$_2$] (**1**) and (b) [V(ac*Cl*bh)$_2$] (**2**) with the atom labeling schemes. All nonhydrogen atoms are represented by their 50% probability thermal ellipsoids.

Table 3. Selected bond parameters[a] (lengths in Å and angles in °) for **1** and **2**.

Complex	**1**	**2**
V−O(1)	1.930(2)	1.931(2)
V−O(2)	1.911(2)	1.902(2)
V−O(3)	1.933(2)	1.939(2)
V−O(4)	1.914(2)	1.920(2)
V−N(1)	2.040(2)	2.042(3)
V−N(3)	2.041(2)	2.035(2)
O(1)−V−O(2)	139.35(8)	138.85(9)
O(1)−V−O(3)	80.71(7)	80.64(9)
O(1)−V−O(4)	86.53(7)	86.32(9)
O(2)−V−O(3)	86.44(8)	86.71(9)
O(2)−V−O(4)	125.23(8)	126.07(9)
O(3)−V−O(4)	140.00(8)	138.70(9)
O(1)−V−N(1)	83.42(8)	83.32(10)
O(1)−V−N(3)	127.72(8)	128.82(9)
O(2)−V−N(1)	74.84(7)	74.94(10)
O(2)−V−N(3)	88.41(8)	87.65(9)
O(3)−V−N(1)	128.40(8)	129.37(9)
O(3)−V−N(3)	83.76(8)	83.16(9)
O(4)−V−N(1)	86.94(8)	87.12(9)
O(4)−V−N(3)	74.53(7)	75.01(9)
N(1)−V−N(3)	141.30(8)	140.69(10)

[a] Selected bond lengths (Å) in the previously reported structure of **1** [19]: V−O(1) = 1.929(7), V−O(2) = 1.920(7), V−O(3) = 1.943(7), V−O(4) = 1.906(8), V−N(1) = 2.031(8), V−N(3) = 2.034(8).

while the distances between the opposing corners of the two trigonal faces are 2.34−2.50 and 2.40−2.50 Å in **1** and **2**, respectively. The torsion angles involving the opposing corners and the centroids of the trigonal faces are 8.4°, 9.2°, and 9.5° for **1** and 7.7°, 7.8°, and 8.0° for **2**. The trigonal twist angles (ϕ) [55,68] calculated by averaging the corresponding torsion angles are 9.0° and 7.8° for **1** and **2**, respectively (figure 3).

3.4. *Redox properties*

Electron transfer properties of **1–4** in DMF were studied using cyclic voltammetry. None of the complexes shows oxidation response in the anodic scan. However, all of them display a reduction response with $E_{1/2}$ values in the potential range −0.16–−0.25 V (*versus* Ag/AgCl) (figure S2, Supplementary material). The peak-to-peak separations (E_p) for this reduction are 110–130 mV (table 2). The one-electron nature of this couple is conjectured by comparing the peak currents with the peak currents of known reversible/quasi reversible one-electron transfer processes under comparable conditions [32,33,39–42,65–67]. Similar reduction response for **1** and other non-oxo vanadium(IV) complexes with tridentate O,N,O-donor ligands observed in dichloromethane using hanging mercury drop electrode or platinum electrode on the cathodic side of Ag/AgCl (−0.02–−0.46 V) has been assigned to V(IV)−V(III) redox process [22]. Further, the redox inactivity of $[\mathrm{V_2O_3}(\mathrm{ac}R\mathrm{bh})_2]$ and the lone V(V)−V(IV) redox couple of $[\mathrm{VO(OMe)}(\mathrm{ac}R\mathrm{bh})]_2$ at a higher potential range [40] compared to that observed for the present complexes supports the above assignment. The trend in the $E_{1/2}$ values of **1–4** clearly reflects the influence of the inductive effect of the substituent (R) present at the *para* position of the aroyl fragment of $\mathrm{ac}R\mathrm{bh}^{2-}$. The potential is the lowest for the most electron-releasing methoxy substituent, while it is the highest for the most electron-withdrawing nitro substituent. There is a

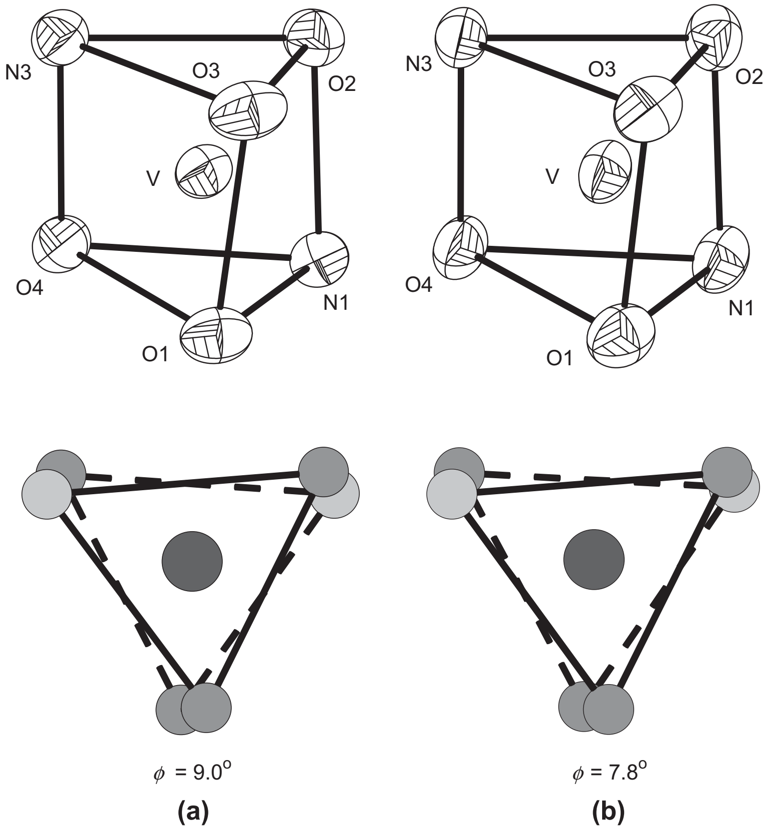

Figure 3. Distorted trigonal prismatic coordination spheres in (a) **1** and (b) **2**: general views (top) and ball and stick diagrams viewed along a trigonal face (bottom).

satisfactory linear relationship of the $E_{1/2}$ values with the corresponding Hammett substituent constants (σ_p) (figure S2). Thus, the increase in the electron-withdrawing character of the substituent facilitates the reduction of the metal center and stabilizes the lower oxidation state. Complex **4** with the ligand containing the most electron-withdrawing nitro group (ac*NO₂*bh^{2-}) displays a second, one-electron reduction response with an $E_{1/2}$ value of $-1.04\,\mathrm{V}$ ($E_p = 240\,\mathrm{mV}$) (figure S2). $\{V_2O_3\}^{4+}$ and $\{VO(OMe)\}^{2+}$ with ac*NO₂*bh^{2-} do not display a redox couple around this potential [40]. Thus, it is very likely that this second electron transfer response in **4** is not ligand–centered, but due to the V(III)−V(II), redox couple.

4. Conclusions

In continuation of our work on vanadium chemistry with Schiff bases involving acid hydrazides, herein we have reported a series of trigonal prismatic non-oxo vanadium(IV) complexes with tridentate acetylacetone aroylhydrazones and their physical properties. The complexes have been synthesized by using a simple method that does not require non-oxo starting material or absence of air or moisture. Electronic spectra of the complexes are comparable and display three bands due to LMCT and ligand-centered transitions. The EPR characteristics of the one-electron paramagnetic complexes are very similar. The frozen solution spectra of each complex are axial and the unpaired electron resides in a hydrid orbital which is predominantly 3d in character. All the complexes are redox active and display a metal-centered redox couple sensitive to the substituent on the ligand. Similar spectroscopic and electrochemical characteristics of the complexes signify their comparable molecular structures. The structures of two representative complexes determined by X-ray crystallography are similar and confirm the distorted trigonal prismatic coordination sphere around the metal center.

Supplementary material

Figures S1 and S2 illustrating electronic spectra of 3 and cyclic voltammogram of 4, respectively. CCDC 865811 and 865812 contain the crystallographic data for **1** and **2**, respectively. These data can be obtained free of charge via www.ccdc.cam.ac.uk/data_request/cif or from the Cambridge Crystallographic Data Center, 12 Union Road, Cambridge, CB2 1EZ, UK; Fax: +44 1223 336 033 or E-mail: deposit@ccdc.cam.ac.uk.

Acknowledgements

Financial support for this work has been received from the Department of Science and Technology (DST) (IYC Grant No. IR/S1/CF-01E/2011). K. Nagaraju and A. Sarkar thank the Council of Scientific and Industrial Research for research fellowships. We thank the DST and the University Grants Commission for the facilities provided under the FIST and the CAS programs, respectively.

References

[1] D. Rehder. *Coord. Chem. Rev.,* **182**, 297 (1999).
[2] A. Butler. *Coord. Chem. Rev.,* **187**, 17 (1999).
[3] C.D. Garner, E.M. Armstrong, R.E. Berry, R.L. Beddoes, D. Collison, J.J.A. Cooney, M. Helliwell. *J. Inorg. Biochem.,* **80**, 17 (2000).
[4] D. Rehder. *J. Inorg. Biochem.,* **80**, 133 (2000).
[5] D.C. Crans, J.J. Smee, E. Gaidamauskas, L. Yang. *Chem. Rev.,* **104**, 849 (2004).
[6] D. Rehder. *Bioinorganic Vanadium Chemistry*, Wiley, Chichester (2008).
[7] T. Hirao. *Coord. Chem. Rev.,* **237**, 1 (2003).
[8] H. Michibata, K. Kanamori, T. Hirao. *Coord. Chem. Rev.,* **255**, 2149 (2011).
[9] T. Hirao. *Chem. Rev.,* **97**, 2707 (1997).
[10] K. Nomura, S. Zhang. *Chem. Rev.,* **111**, 2342 (2011).
[11] K.H. Thompson, J.H. McNeill, C. Orvig. *Chem. Rev.,* **99**, 2561 (1999).
[12] K.H. Thompson, C. Orvig. *Coord. Chem. Rev.,* **219–221**, 1033 (2001).
[13] H. Sakurai, Y. Kojima, Y. Yoshikawa, K. Kawabe, H. Yasui. *Coord. Chem. Rev.,* **226**, 187 (2002).
[14] E.M. Page. *Coord. Chem. Rev.,* **172**, 111 (1998).
[15] M.R. Maurya. *Coord. Chem. Rev.,* **237**, 163 (2003).
[16] D.C. Crans. *Pure Appl. Chem.,* **77**, 1497 (2005).
[17] F. Avecilla, P. Adão, I. Correia, J.C. Pessoa. *Pure Appl. Chem.,* **81**, 1297 (2009).
[18] J.R. Fulton. *Annu. Rep. Prog. Chem., Sect. A*., **107**, 152 (2011).
[19] A.A. Diamantis, M. Manikas, M.A. Salam, M.R. Snow, E.R.T. Tiekink. *Aust. J. Chem.,* **41**, 453 (1988).
[20] U. Auerbach, B.S.P.C.D. Vedova, K. Weighardt, B. Nuber, J. Weiss. *J. Chem. Soc., Chem. Commun*., 1004 (1990).

[21] M.A.A.F. de C.T. Carrondo, M.T.L.S. Duarte, J.J.R. Frausto da Silva, J.A.L. da Silva. *Struct. Chem.*, **3**, 113 (1992).
[22] W. Mickler, A. Mönner, H. Hefele, E. Ludwig, E. Uhlemann. *Electrochim. Acta,* **42**, 421 (1997).
[23] T.K. Paine, T. Weyhermüller, E. Bill, E. Bothe, P. Chaudhuri. *Eur. J. Inorg. Chem.,* **4299**, (2003).
[24] T.K. Paine, T. Weyhermuller, L.D. Slep, F. Neese, E. Bill, E. Bothe, K. Wieghardt, P. Chaudhuri. *Inorg. Chem.,* **43**, 7324 (2004).
[25] M. Sutradhar, G. Mukherjee, M.G.B. Drew, S. Ghosh. *Inorg. Chem.,* **46**, 5069 (2007).
[26] N. Sharma, Meena, M. Thakur, V. Kumar, S.C. Chaudhry. *Indian J. Chem*., 47A, 685 (2008).
[27] K.C.M. Westrup, T. Gregório, D. Stinghen, D.M. Reis, P.B. Hitchcock, R.R. Ribeiro, A. Barison, D.F. Back, E.L. de Sá, J.F. Soares. *Dalton Trans.,* **40**, 3198 (2011).
[28] T. Kajiwara, R. Wagner, E. Bill, T. Weyhermüller, P. Chaudhuri. *Dalton Trans*., 40, 12719 (2011) and references therein.
[29] Y. Jin, M.S. Lah. *Eur. J. Inorg. Chem.,* **4944**, (2005).
[30] N. Sharma, M. Kumari, V. Kumar, S.C. Chaudhry, S.S. Kanwar. *J. Coord. Chem.,* **63**, 176 (2010).
[31] N. Sharma, M. Thakur, S.C. Chaudhry. *J. Coord. Chem.,* **63**, 1228 (2010).
[32] N.R. Sangeetha, V. Kavita, S. Wocadlo, A.K. Powell, S. Pal. *J. Coord. Chem.,* **51**, 55 (2000).
[33] N.R. Sangeetha, S. Pal. *Bull. Chem. Soc. Jpn.,* **73**, 357 (2000).
[34] S.N. Pal, S. Pal. *J. Chem. Crystallogr.,* **30**, 329 (2000).
[35] S.N. Pal, S. Pal. *Acta Crystallogr., Sect. C*., 57, 141 (2001).
[36] S.N. Pal, K.R. Radhika, S. Pal. *Z. Anorg. Allg. Chem.,* **627**, 1631 (2001).
[37] A. Sarkar, S. Pal. *Polyhedron,* **25**, 1689 (2006).
[38] A. Sarkar, S. Pal. *Polyhedron,* **26**, 1205 (2007).
[39] A. Sarkar, S. Pal. *Inorg. Chim. Acta,* **361**, 2296 (2008).
[40] A. Sarkar, S. Pal. *Inorg. Chim. Acta,* **362**, 3807 (2009).
[41] A. Sarkar, S. Pal. *Eur. J. Inorg. Chem.,* 622 (2009).
[42] A. Sarkar, S. Pal. *Eur. J. Inorg. Chem.,* 5391 (2009).
[43] R.A. Rowe, M.M. Jones. *Inorg. Synth.,* **5**, 113 (1957).
[44] G.A. Bain, J.F. Berry. *J. Chem. Educ.,* **85**, 532 (2008).
[45] Bruker-Nonius Analytical X-ray Systems Inc. *SMART V5.630 and SAINT-plus V6.45*, Madison, Wiskonsion, USA (2003).
[46] G.M. Sheldrick. *SADABS, Program for Area Detector Absorption Correction*, University of Göttingen, Göttingen, Germany (1997).
[47] G.M. Sheldrick. *SXHELX-97, Programs for the Crystal Structure Analysis*, University of Göttingen, Göttingen, Germany (1997).
[48] L.J. Farrugia. *J. Appl. Crystallogr.,* **32**, 837 (1999).
[49] P. McArdle. *J. Appl. Crystallogr.,* **28**, 65 (1995).
[50] A.L. Spek. *PLATON, A Multipurpose Crystallographic Tool*, Utrecht University, Utrecht, The Netherlands (2002).
[51] M. Rangel, A. Leite, M.J. Amorim, E. Garribba, G. Micera, E. Lodyga-Chruscinska. *Inorg. Chem.,* **45**, 8086 (2006).
[52] A. Mukhopadhyay, S. Pal. Eur. *J. Inorg. Chem*., 4879 (2006) and references therein.
[53] W. Kemp. *Organic Spectroscopy*, pp. 56–66, Macmillan, Hampshire (1987).
[54] D. Sanna, V. Ugone, G. Micera, E. Garribba. *Dalton Trans*., **41**, 7304 (2012) and references therein.
[55] A. Desideri, J.B. Raynor, A.A. Diamantis. *J. Chem. Soc., Dalton Trans*., 423 (1978).
[56] A.A. Diamantis, J.B. Raynor, P.H. Rieger. *J. Chem. Soc., Dalton Trans*., 1731 (1980).
[57] W.-L. Kwik, E.I. Stiefel. *Inorg. Chem.,* **12**, 2337 (1973).
[58] A. Jezierski, J.B. Raynor. *J. Chem. Soc., Dalton Trans*., 1 (1981).
[59] R.M. Olk, W. Dietzsch, R. Kirmse, J. Stach, E. Hoyer, L. Golič. *Inorg. Chim. Acta,* **128**, 251 (1987).
[60] M. Branca, G. Micera, A. Dessì, D. Sanna, K.N. Raymond. *Inorg. Chem.,* **29**, 1586 (1990).
[61] A. Dessì, G. Micera, D. Sanna, L.S. Erre. *J. Inorg. Biochem.,* **48**, 279 (1992).
[62] P.R. Klich, A.T. Daniher, P.R. Challen, D.B. McConville, W.J. Youngs. *Inorg. Chem.,* **35**, 347 (1996).
[63] B. Morgenstern, S. Steinhauser, K. Hegetschweiler, E. Garribba, G. Micera, L. Nagy. *Inorg. Chem.,* **43**, 3116 (2004).
[64] A. Choudhury, B. Geetha, N.R. Sangeetha, V. Kavita, V. Susila, S. Pal. *J. Coord. Chem.,* **48**, 87 (1999).
[65] G.V. Karunakar, N.R. Sangeetha, V. Susila, S. Pal. *J. Coord. Chem.,* **50**, 51 (2000).
[66] N.R. Sangheeta, C.K. Pal, P. Ghosh, S. Pal. *J. Chem. Soc., Dalton Trans*., 3293 (1996).
[67] S.N. Pal, S. Pal. *J. Chem. Soc., Dalton Trans*., 2102 (2002).
[68] E.I. Stiefel, G.F. Brown. *Inorg. Chem.,* **11**, 434 (1972).